Journal of Biotechnology 414 (2026) 153–162

Contents lists available at ScienceDirect

Journal of Biotechnology

journal homepage: www.elsevier.com/locate/jbiotec

Autotrophic isopropanol production by *Cupriavidus necator* using industrial biogas and incinerator flue gases as carbon sources

I. Weickardt [a], A. Zhang [a], E. Lombard [a], E. Grousseau [b], L.M. Blank [c,d], C. Chenebault [e], B. Percheron [e], N. Gorret [a], S.E. Guillouet [a,*]

[a] Toulouse Biotechnology Institute (TBI), Université de Toulouse, CNRS, INRAE, INSA, Toulouse, France
[b] IATE, University of Montpellier, INRAE, Institut Agro, Montpellier, France
[c] iAMB - Institute of Applied Microbiology, ABBt - Aachen Biology and Biotechnology, BioSC, RWTH Aachen University, Aachen, Germany
[d] WSS center catalaix, France
[e] Suez, CIRSEE, Le Pecq, France

ARTICLE INFO

Keywords:
Cupriavidus
Carbon Dioxide
Gas fermentation
Isopropanol
Biogas
Flue gas

ABSTRACT

Gas fermentation is a promising approach to reduce carbon emissions of production processes by using microorganisms to convert industrial gas streams into valuable carbon-based products. Here, isopropanol production by engineered *Cupriavidus necator* from CO_2-rich gas streams is presented. Four different engineered strains were tested first on synthetic gas mixture, and one was selected, namely Re2133/pEG7d, for further evaluation on two different industrial CO_2-rich gas streams. Up to 1.6 g L^{-1} of isopropanol was obtained in autotrophic gas flasks with this strain. Then, raw biogas from landfill containing 45% methane was successfully used as a CO_2 source for isopropanol production with this strain Re2133/pEG7d producing up to 2.35 ± 0.25 g L^{-1}, and methane enrichment was demonstrated. Finally, flue gases from a municipal incinerator were used as a source of CO_2 and O_2 for the autotrophic cultivation of the strain Re2133/pEG7d, obtaining a final isopropanol concentration of 2.5 ± 0.3 g L^{-1}.

This work highlighted the robustness of *C. necator* to potential industrial gas stream impurities and its versatility in using diverse gaseous feedstocks, promising future developments at larger scale.

1. Introduction

To reach the climate goals for 2050, anthropogenic greenhouse gas emissions have to be reduced drastically, shifting from fossil resources to sustainable alternatives and moving towards a circular economy. It is essential to meet the demand for carbon-based industrial products with alternative, low-emission processes. This comprises recirculating carbon that would otherwise be emitted as CO_2, thereby contributing to climate change. One promising approach is gas fermentation, where microorganisms convert carbon to produce a wide range of value-added products.

The relevance of different microbial conversion processes is determined by the composition of the gas streams. Acetogens are efficient biocatalysts for gas streams rich in carbon monoxide and free of oxygen, while Knallgas bacteria can effectively convert streams containing carbon dioxide, such as flue gas from the cement industry and lime production (Nagappan et al., 2020, Patricio et al., 2017). While gas streams with high purity carbon dioxide are already directly being valorised in industry, the separation of carbon dioxide from streams additionally containing, e.g., nitrogen is costly (Patricio et al., 2017, Kircher and Schwarz, 2023). For example, biogas from landfill before upgrading, typically contains 45–70% CH_4 and 30–40% CO_2 (Hagen et al., 2001). To introduce methane into the gas grid, a purity of 95% is required, with the cost of separating CH_4 from CO_2 being inversely proportional to the amount of CO_2 present (Kircher and Schwarz, 2023). In case of incinerator flue gas, the composition typically contains around 5–11% CO_2, 8–12% O_2 and 80% N_2 depending on the process conditions and the waste composition (Aouini et al., 2014, Patricio et al., 2017). In 2018, incinerator plants in Europe emitted around 78 Mt CO_2, with around 55% CO_2 being of fossil origin (Warringa, 2021). The

* Corresponding author.
E-mail addresses: isabell.weickardt@insa-toulouse.fr (I. Weickardt), azhang@insa-toulouse.fr (A. Zhang), elombard@insa-toulouse.fr (E. Lombard), estelle.grousseau@umontpellier.fr (E. Grousseau), lars.blank@rwth-aachen.de (L.M. Blank), celia.chenebault@suez.com (C. Chenebault), benjamin.percheron@suez.com (B. Percheron), ngorret@insa-toulouse.fr (N. Gorret), guillouet@insa-toulouse.fr (S.E. Guillouet).

https://doi.org/10.1016/j.jbiotec.2026.03.005
Received 11 December 2025; Received in revised form 2 March 2026; Accepted 6 March 2026
Available online 8 March 2026

valorisation of carbon dioxide in incinerator flue gas is challenging due to fluctuations in gas composition based on the processed waste (Aouini et al., 2014). The low CO_2 content in incinerator gas results in higher energy requirements for carbon capture. Microbial processes offer an inherent advantage over chemical methods due to their higher flexibility regarding feedstock composition and greater tolerance to impurities (Mohammadi et al., 2011, Liew et al., 2013).

Among the Knallgas bacteria, *Cupriavidus necator* has attracted most interest due to its versatile metabolism allowing for hetero- and autotrophic growth under aerobic and anaerobic conditions. Furthermore, it is characterised by the ability to redirect substantial carbon flux toward the storage molecule PHA. This characteristic has been exploited by replacing the PHA biosynthesis with heterologous pathways. Additionally, proof-of-concept studies have successfully demonstrated the production of PHA based on syngas (Volova and Voinov, 2004), high-purity off-gas from an ethanol plant (Garcia-Gonzalez and Wever, 2017, Rossi et al., 2025), and biogas (Garcia-Gonzalez and Wever, 2017, Serna--García et al., 2024). Also, the first heterologous product, lycopene, has been produced using the off-gas stream from a coal-fired plant (Wu et al., 2022). In this study, this is complemented by demonstrating the potential for producing the biofuel isopropanol as an additional heterologous product. We focus on a direct comparison of cultivations using industrial-grade gas sources and pure lab-grad gasses.

Isopropanol is the most widely used disinfectant world-wide due to its antimicrobial properties (Rosenberg et al., 2013). Its high-octane number and energy density make it an interesting add-in for biofuels. Additionally, it is commonly used as solvent, e.g., in the cement industry, in cosmetics and healthcare products. In the chemical industry, isopropanol is furthermore used as a feedstock for the production of acetone, polypropylene, acrylates, and isopropylamines (Logsdon and Loke, 2000, Rosenberg et al., 2013). The conventional production process via direct or indirect hydration of propene relies on propene, which is a fossil-derived product (Logsdon and Loke, 2000).

While some acetogens can produce isopropanol natively, higher concentrations and lower by-product formation and faster growth rates have been obtained by heterologously expressing genes from *Clostridium* sp. in other host organisms. The highest isopropanol concentration so far was obtained under heterotrophic conditions with *Escherichia coli* with 40 g L^{-1} in the liquid phase using glucose as substrate (Inokuma et al., 2010). However, for the valorisation of gaseous substrates, the most advanced productions have been obtained anaerobically in engineered *Clostridium autoethanogenum* with 8 g L^{-1} from syngas (Liew et al., 2022) and aerobically in engineered *C. necator* with concentrations ranging 8–11.5 g L^{-1} from CO_2 (Di Bisceglie et al., 2025; Weickardt et al., 2025, unpublished).

A wide range of promoters has been used in *C. necator*. As for the cell-toxic product isopropanol reduced growth rates were reported when the operon was controlled by a constitutive promoter, inducible-systems are preferred (Grousseau et al., 2014). The main disadvantage of inducible promoter is the high cost of the inducer molecule on an industrial scale (Johnson et al., 2018). This makes auto-inducible systems attractive, which are upregulated under nutrient limitation or a switch of substrate. Several auto-inducible promoters have been successfully applied in *C. necator*, including P_{phaP} (Srinivasan et al., 2002, Fukui et al., 2011), P_{cbbL} (Lütte et al., 2012, Dangel and Tabita, 2015) as well as P_{acoD} and P_{acoX} (Delamarre and Batt, 2006, Schwarze et al., 2010). The strongest native promoters identified so far is P_{SH}, which is induced on glycerol and under autotrophic conditions (Jugder et al., 2016). Here isopropanol production was performed autotrophically on four different engineered strains, a constitutive isopropanol producer and three inducible producers responding to the arabinose or rhamnose promoter and to an auto-induced promoter under nitrogen limitation. One of the strains was further evaluated for growth and production on two industrial flue gases, a biogas from landfill and an incinerator flue gas.

2. Material and methods

2.1. Plasmid and strain construction

Four different isopropanol-producing strains were used, which all contained the isopropanol-operon (Grousseau et al., 2014) in the PHA deletion mutant Re2133 ΔphaB1B2B3C1 (Budde et al., 2011) but under different promoter (Table 1; Fig. 1). The isopropanol operon comprises the native phaA (H16_A1438) and ctfAB (H16_A1331, H16_A1332) and codon-optimised acetoacetate decarboxylase (CA_P0165) from *Clostridium acetobutylicum* and codon-optimised alcohol dehydrogenase (AF157307) from *Clostridium beijerinckii*. In strain Re1233/pEG7b the operon was placed downstream of the constitutive P_{TAC} promoter. In Re1233/pEG7c it was placed under the control of the arabinose-inducible P_{Bad} promoter (Grousseau et al., 2014) and in Re2133/pJLSG02 under the control of the rhamnose-inducible promoter P_{Rha}. In strain Re2133/pEG7d, the operon was inserted downstream of the P_{Gln} promoter (a 400 bp upstream sequence of the glutamine synthetase glnA3 gene (H16_B2191), a putative NtrC binding site). So far, nitrogen-dependent systems have been successfully established in *E. coli*, using the glnA2 promoter for the expression of recombinant proteins (Schroeckh et al., 1996).

DNA sequence amplification was achieved using Phusion High-Fidelity PCR Master Mix with GC Buffer (New England Biolabs, Ipswich, MA, USA). QIAQuick Gel Extraction Kit (QIAGEN, Valencia, CA, USA) was used for gel purification of all DNA products. Plasmid extractions were carried out using the QIAprep Spin Miniprep Kit (QIAGEN). Restriction enzymes used were from New England Biolabs.

For strain construction, the protocol described by Grousseau et al., 2014 was followed. In short, the promoter region of the broad-host vector pBBR1MCS-2 (Kovach et al., 1995) was replaced with the P_{gln} promoter. For construction of pEG7d, the 5′-OL pBBR1MCS-2 *glnA3_up* and 3′-OL *glnA3_up* pBBR1MCS-2 primers described in Table 2 were used to amplify the 400 bp upstream sequence of glnA3 gene (H16_B2191). The 5′-OL *glnA3_ up* pBBR1MCS-2 and 3′-OL pBBR1MCS-2 *glnA3_up* primers were used to amplify the plasmid backbone pBBR1MCS-2. Both fragments were assembled by one-step isothermal DNA assembly protocol (Gibson et al., 2009) to lead to pBBR1MCS-2-PGln. Then pBBR1MCS-2-PGln digested by *Cla*I and *Xho*I was used respectively as backbone DNA for the assembly of pEG7d plasmid. The fragment with pathway genes from the digestion of pEG7a (Grousseau et al., 2014) with *Xho*I and *Cla*I was isolated and purified. The fragment was then ligated with the corresponding digested vector to obtain pEG7d plasmid.

For construction of pSLSG02, the Rhamnose promoter was amplified from pKRrha plasmid (Sydow et al., 2017) with the primers pBBad_Prha_fw and pBBad_Prha_rev (Table 2). The fragment was ligated with a DNA sequence amplified from pBBAD with pBBad_ampli_Fw and pBBad_ampli_rev primers. Both fragments were assembled by one-step isothermal DNA assembly protocol (Gibson et al., 2009) to lead to pBBAD-PGln. The fragment with pathway genes from the digestion of pEG7a (Grousseau et al., 2014) with *Xho*I and *Eco*RV was isolated and purified. The fragment was then ligated with the corresponding digested

Table 1
Plasmids used in this study.

Plasmid	Description	Literature
pEG7b	pBBR1MCS-2[Kanr]-[Ptac-*phaA*-RBS-*ctfAB*-RBS-*adc**-RBS-*adh**]	(Grousseau et al., 2014)
pEG7c	pBBR1MCS-2[Kanr]-[PBad-*phaA*-RBS-*ctfAB*-RBS-*adc**-RBS-*adh**	Grousseau et al., (2014))
pJLSG02	pBBR1MCS-2[Kanr]-[Prha-*phaA*-RBS-*ctfAB*-RBS-*adc**-RBS-*adh**]	This work
pEG7d	pBBR1MCS-2[Kanr]-[Pgln-*phaA*-RBS-*ctfAB*-RBS-*adc**-RBS-*adh**]	This work

(*) the gene was codon-optimised.
The RBS sequence was AAAGGAGGACAACC (Lu et al., 2012)

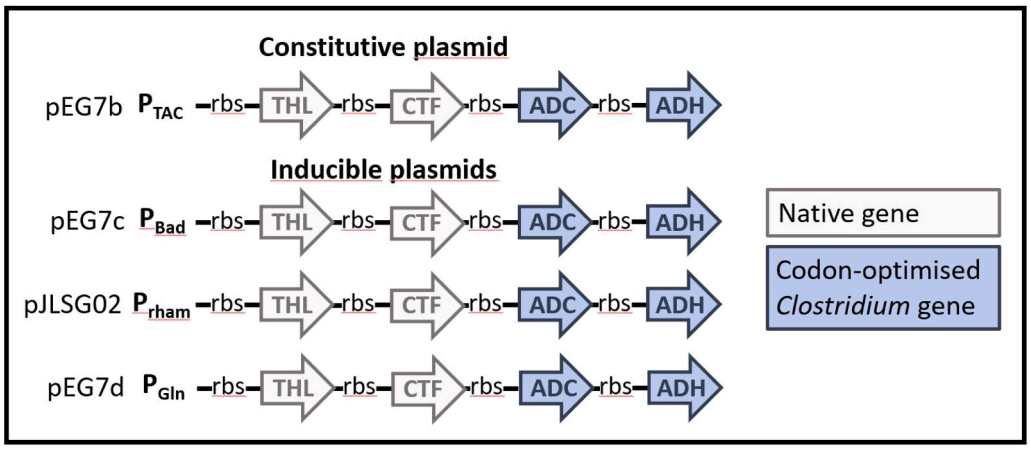

Fig. 1. Schematic representation of the isopropanol biosynthetic operon inserted in the plasmid pBBR1MCS-2. Each plasmid was incorporated into strain Re2133 (H16 ΔphaB1B2B3C1, Budde et al. 2011). Plasmid name, promoter (in bold), genes name in arrows.

Table 2
Primers used for pBBR1MCS-2-PGln construction.

Primer name	Sequence (5' to 3')
Construction of pBBR1MCS-2-PGln	
5'-OL pBBR1MCS-2 *glnA3_up*	GCTCACTCATTAGGCACCCCAGGCCATCGTACTTGCTGAACAGCACC
3'-OL *glnA3_up* pBBR1MCS-2	GGTGCTGTTCAGCAAGTACGATGGCCTGGGGTGCCTAATGAGTGAGC
5'-OL *glnA3_ up* pBBR1MCS-2	CAAAGTCGGAAGGAGCCGATCCGGTACCGGGCCCCCCCTC
3'-OL pBBR1MCS-2 *glnA3_up*	CGAGGGGGGGCCCGGTACCGGATCGGCTCCTTCCGACTTT
Construction of pBBAD-PRham	
pBBad_Prha_fw	ATTGTCTGATTCGTTACCAATTAATCTTTCTGCGAATTGAG
pBBad_Prha_rev	CTAGCCCAAAAAAACGGGTTACGACCAGTCTAAAAAGCG
pBBad_ampli_Fw	CGCTTTTTAGACTGGTCGTAACCCGTTTTTTTGGGCTAG
pBBad_ampli_rev	CTCAATTCGCAGAAAGATTAATTGGTAACGAATCAGACAAT

vector to obtain pJLSG02 plasmid.

The ligation products were transformed into chemical competent *E. coli* Top10 cells (InvitrogenTM, Life technologies). After plasmid extraction, their correct assembly was verified via plasmid digestion. The correct gene insertion into the plasmids was confirmed via sequencing. Every correct plasmid was transformed into *E. coli* S17–1 by electroporation, which was then used for conjugative transfer of the plasmid into *C. necator* Re 2133.

2.2. Medium and preculture

Strains were streaked from a glycerol stock being stored at −70°C on complex medium plates. After three days of incubation, one colony was used to inoculate 10 mL of complex medium in a baffled 50 mL shake flask. The cells were grown to an OD of around 1.0 (~17 h) and used to inoculate a second preculture with an OD of 0.05 in minimal medium. This was conducted in 50 mL liquid containing 2 g L^{-1} fructose and 0.5 g L^{-1} NH_4Cl in 250 mL baffled shake flask. After this preculture reached an OD of around 0.5 it was used to inoculate the main cultivation with an OD of 0.05.

The rich medium contained 27.5 g L^{-1} dextrose-free Bacto™ Tryptic soy, supplemented with 20 g L^{-1} agar for plate cultivation. The minimal medium contained 11.6 g L^{-1} Na_2HPO_4 x 12 H_2O, 5.2 g L^{-1} NaH_2PO_4 x 2 H_2O, 0.8 g L^{-1} $MgSO_4$ x 7 H_2O, 0.08 g L^{-1} $CaCl_2$ x 2 H_2O, 0.45 g L^{-1} K_2SO_4, 0.04 g L^{-1} NaOH, 0.033 mg L^{-1} $NiCl_2$ x 6 H_2O, 15 mg L^{-1} $FeSO_4$ x 7 H_2O, 2.4 mg L^{-1} $MnSO_4$ x H_2O, 2.4 mg L^{-1} $ZnSO_4$ x 7 H_2O and 0.48 mg L^{-1} $CuSO_4$ x 5 H_2O. In the mid-exponential growth phase additional 0.033 mg L^{-1} $NiCl_2$ x 6 H_2O were added to the cultivation. For main cultivations, 1.0 g L^{-1} NH_4Cl were added, limiting the maximal obtainable cell dry weight to 2 g L^{-1}, corresponding to an OD of 1.0. For heterotrophic cultivations, 30 g L^{-1} fructose were added, for lithoautotrophic growth, no organic carbon source was added. In all cultivations, 10 mg L^{-1} gentamicin and 100 mg L^{-1} kanamycin were added. For induction 1 g L^{-1} L-arabinose or 0.5 g L^{-1} L-rhamnose were added in the mid-exponential growth phase except stated otherwise.

2.3. Main culture

All flasks were incubated at 30°C and 140 rpm. For autotrophic cultivations, baffled Schott bottles closed with a hermetic lid were used. In the lower part of the bottles, a glass nozzle with a silicon septum was attached to enable sampling. The lid was equipped with two valves, for connections with the gas refill system, the barometer to measure headspace pressure, the vacuum pump or a syringe for gas sampling as described in Weickardt et al., 2025. Incinerator cultivations were conducted with 50 mL liquid volume to reduce gas consumption due to limited available amount, while for biogas cultivations 100 mL cultivation volume was used.

The bottle headspace was filled with the envisaged gas mixture. First, the headspace was emptied by applying a vacuum. Strain characterisations were conducted with a commercial gas mixture (UN 1954 compressed gas, flammable, N.O.S. (Hydrogen, Carbon dioxide), 2.1, (B/D), Air Liquide, Bagneux, France) containing 80.12% hydrogen and 19.88% carbon dioxide. This mixture was filled up to an overpressure of 2.3 bar. 0.2 bar oxygen were added, to reach a final gas composition of $H_2/O_2/CO_2$ 74/8/18 mol% (Weickardt et al., 2025). During the cultivation, the headspace-pressure was followed. The gas phase was replaced by a new gas mixture when the over-pressure dropped to around 0.8 bar.

Depending on the composition of the off-gas, the headspace of the cylinder was topped up after being filled with industrial gas with the appropriate gas to achieve the targeted mixture composition. To add H_2 and adjust CO_2 quantity in cultivations with industrial gas and their references, pure carbon dioxide or hydrogen (Air Liquid, Bayeux,

France) instead of the commercial CO_2/H_2-mixture was used. The cultivations for testing the impact of methane were conducted with pure methane (AirLiquide, purity > 99.9995%, Bagneux, France). The bottles were first filled with the off-gas and then completed with the necessary pure gases to reach the targeted mixture and a final pressure of 2.3–2.5 bars. Pure oxygen was supplied to reach the 8–12% range to avoid hydrogenases inhibition by the oxygen and hydrogen was supplied the most (30–45% range) because it has the lowest solubility of the three gases (Di Bisceglie et al., 2024; Weickardt et al., 2025).

To test the transfer of volatile fatty acids from the biogas into the cultivation medium, triplicates were conducted in non-inoculated minimal medium without nitrogen source. The bottle headspace was filled with 40% industrial biogas, 50% H_2 and 10% O_2 and incubated for 70 h at 30°C and 140 rpm to simulate cultivation conditions.

During experiments using industrial off-gas and their respective reference cultivations, before and after the gas refill, the headspace composition was analysed. For this, 10 mL of the headspace gas was sampled via a syringe equipped with a 3-way-valve and directly injected into a GC-MS.

2.4. Analytical methods

Growth was followed by measuring the optical density (OD) with a Hach Lange Spectrophotometer (Hach Lange Berlin, DR3900) with 2 mm-length glass cuvettes. If necessary, samples were diluted with tap water. The correlation to the cell dry weight was determined as CDW = 2 x OD.

Concentrations of fructose, isopropanol, acetone, pyruvate, succinate, acetate, arabinose and rhamnose were measured via HPLC from the filtered supernatant of samples centrifuged for 5 min at 13 200 rpm. A HPLC Waters e2695 (Waters, Milford, US) with a 300 × 7.8 mm HPX-87H Biorad Aminex column was used, equipped with a 30 × 4.6 mm Cation H^+ cartridge pre-column (Bio-Rad, Hercules, CA, USA), and a refractive Index (RI) and UV detector. Analysis were conducted with 50 °C column temperature and 2.5 mM H_2SO_4 as eluent with a flow rate of 0.5 mL min^{-1}.

The headspace composition was determined offline using gas chromatography. Gas samples of 10 mL were taken from the bottle headspace using a 10 mL syringe closed with a 3-way valve, in front of which a syringe filter was attached. The syringe was connected to the bottle lid via a 10 cm tube. The gas samples were injected into the GC to quantify H_2, CO_2, O_2, N_2 and CH_4. The used device was the gas chromatograph Trace 1300, Thermo Scientific (Waltham, USA) equipped with a Rxi-1ms column (30 m, internal diameter 0.32 mm, from Restek, Bellefonte, USA). A loop for hydrogen was implemented using nitrogen as the carrier gas and a pulsed flame photometric detector, while helium was used as carrier gas for quantification of nitrogen, CO_2, O_2 and CH_4, using a thermoconductivity detector.

The concentrations of acetate, propionate, iso-butyrate, butyrate and iso-valerate were measured using a GC-FID from the filtered liquid phase, with 1 g L^{-1} 2-ethylbutyrate in 4.25% orthophosphoric acid as internal standard. Analysis were conducted using a Varian 430-GC gas chromatograph (Agilent Technologies, Santa Clara, USA), which was equipped with a 15 m x 0.53 mm polyethylene glycol column (CP-WAX 58 FFAP CB, Agilent). The carrier gas was nitrogen at a flow rate of 25 mL min^{-1}. Injections were conducted at 250 °C and the program for separation was as followed: 2 min at 90 °C, increase of 20 °C min^{-1} until reaching 130 °C, which was held for 12 min and then decreased by 50 °C min^{-1}up to 210 °C, which was maintained for 2 min. Detection was carried out at 240 °C using a flame ionisation detector (FID).

2.5. Industrial off-gas

Incinerator flue gas and biogas were provided by SUEZ (Le Pecq, France). The biogas was taken from a landfill and filled into 10 L Tedlar gas bags (SKC, Ref. 262–10). The gas contained around 45% CH_4, 37% CO_2, 2.4% O_2 and nitrogen. In the most recent analysis of the biogas composition before sampling, the concentration of total siloxane was 19.5 mg m^{-3}, primarily consisting of trimethylsilanol and hexamethyldisiloxane, as well as 1100 mg m^{-3} total volatile organic compounds which were not further specified. The gas also contained 10–20 ppm CO. Since the biogas sample was taken after the first purification step, it did not contain H_2S.

The flue gas was originated from a municipal incinerator plant (France) processing 4.2 tons of waste per hour, composed of 81% household waste and 19% industrial waste. The off-gas contained 13–19% humidity and the dry gas was composed of around 79% nitrogen, 7% carbon dioxide, and 14% oxygen (Table 3). Further gas impurities are listed in Table 1. The composition provided here was measured by SUEZ (Le Pecq, France) at the time of taking gas samples for the cultivations in this work. Gas was sampled at the plant chimney by filling the gas samples into 6 L stainless steel cannisters under vacuum (Eurofins, Ref. N807W).

3. Results and discussion

3.1. Strain characterisation

Three inducible strains were screened and compared with the constitutive isopropanol producer Re2133/pEG7b (isopropanol operon under constitutive P_{Tac} promoter) (Fig. 2). The three inducible strains differed in the nature of the inducible promoter inserted in front of the isopropanol synthetic operon; the arabinose inducible promoter P_{BAD} (strain Re2133/pEG7c), the rhamnose inducible promoter PRha (Re2133/pJLSG02) and the nitrogen sensitive promoter P_{Gln} (Re2133/pEG7d) (Fig. 1).

Growth rates were twice as high when fructose was used as the carbon source compared to CO_2. In heterotrophic cultivations, Re2133/pEG7c and Re2133/pEG7d obtained the highest growth rates of 0.26 h^{-1} compared the two other strains (0.20 h^{-1}). However, under autotrophic conditions, all four strains achieved an identical growth rate of 0.09 ± 0.01 h^{-1}. With the constitutive strain, (Re2133/pEG7b) already 1.1–1.3 g L^{-1} isopropanol was formed by the end of the growth phase in heterotrophic conditions and 0.2–0.3 g L^{-1} in autotrophic conditions. In contrast, with the three inducible strains, growth and product formation were decoupled as expected.

Overall, the constitutive strain Re2133/pEG7b obtained the highest isopropanol concentrations, reaching 2.4–3.6 g L^{-1} under heterotrophic and 1.2–3.1 g L^{-1} isopropanol under autotrophic conditions. In

Table 3
Composition of incinerator flue gas. (A) Measures at the collect point during filling cannisters performed every minute for 9 h, (B) Semestrial measures of the facility (triplicates).

Compound	Concentration (on dry gas)
A) Average measures during filling cannisters	
N_2	78.5% ± 0.6
CO_2	7,5% ± 0.3
O_2	14% ± 0.3
Humidity	15% ± 1.5
Dust	0.09 mg m^{-3}
NO	94 mg m^{-3} ± 36
N_2O	8 mg m^{-3} ± 2
NH_3	8.4 mg m^{-3} ± 0.3
CO	5.7 mg m^{-3} ± 0.2
SO_2	2.7 mg m^{-3} ± 0.1
Hg	0.002 mg m^{-3} ± 0.0005
B) Average semestrial measures at the incinerator facility	
Total organic carbon	1.1 mg m^{-3}
NOx (eq. NO_2)	159 mg m^{-3} ± 14
Zn	0.03 mg m^{-3} ± 0.01
Total metals (As, Cd, Co, Cr, Cu, Mn, Ni, Pb, Sb, Se, Zn, Te, Tl, V)	0.014 mg m^{-3} ± 1.7

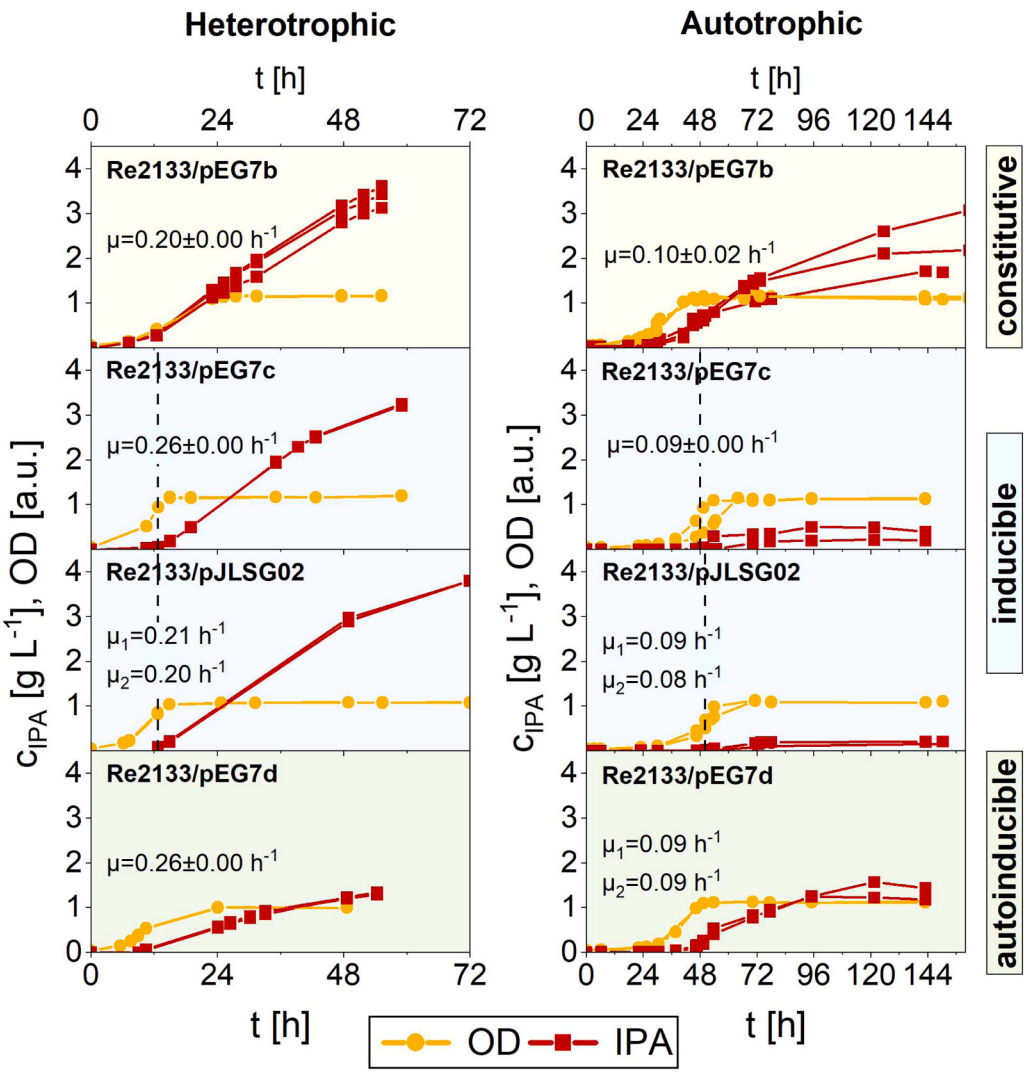

Fig. 2. Isopropanol-formation by four engineered *C. necator* strains under heterotrophic and autotrophic conditions. All strains included the same isopropanol operon, consisting of a native keto-thiolase *thl* and CoA-transferase *ctf*, along with heterologous acetoacetate decarboxylase and alcohol dehydrogenase from Clostridium sp. In strain Re2133/pEG7b, the operon was under the control of the constitutive P_{TAC} promoter, in Re2133/pEG7c of the arabinose-inducible P_{Bad} promoter, in Re2133/pJLSG02 of the rhamnose-inducible P_{rhaB} promoter and in Re2133/pEG7d of the autoinducible P_{Gln} promoter. For autotrophic cultivations, a gas composition of 74% H_2, 8% O_2, 18% CO_2 was used; heterotrophic cultivations were conducted with 30 g L^{-1} fructose. Vertical dashed lines indicate the induction with 0.5 g L^{-1} rhamnose for pJLSG02 and 1 g L^{-1} arabinose for Re2133/pEG7c. Cultivations were performed in triplicate for Re2133/pEG7b and duplicates for the other strains. Maximal specific growth rates are given accordingly: μ_1 and μ_2 values for duplicates; mean of μ + /- standard deviation for triplicates.

contrast, the inducible strains Re2133/pEG7c and Re2133/pJLSG02 were only performant with fructose as substrate with final isopropanol concentrations of 3.2 and 3.8 g L^{-1}, respectively. Under autotrophic conditions, both strains started producing isopropanol after adding the inducer. However, product formation stopped once the growth phase ended due to nitrogen depletion, leading to a low final isopropanol concentration of 0.5 and 0.2 g L^{-1}, respectively. With a two-fold increase in the initial nitrogen concentration, isopropanol formation was prolonged in strain Re2133/pEG7c until growth stopped again (Supplementary Fig. 1). A relation between product formation and nitrogen availability under autotrophic conditions has been shown for the inducible strain, at least for Re2133/pEG7c.

The auto-inducible Re2133/pEG7d, containing the P_{gln} promoter, was cultivated under hetero- and autotrophic conditions. Without the need for added inducer, isopropanol formation started when growth stopped due to nitrogen depletion. Under heterotrophic conditions, the strain showed a lower production than the other three strains, with a final isopropanol concentration of 1.3 ± 0.03 g L^{-1}. Under autotrophic conditions, isopropanol formation started after growth stopped and slowed down only after 120 h, resulting in a final concentration of 1.2–1.6 g L^{-1} and a distinct separation of growth and product formation phase. The strain did not show the previously phenomenon described for strains induced by arabinose or rhamnose of stopping isopropanol formation once nitrogen was depleted.

In previous studies, P_{Bad} and P_{Rham} have been successfully applied for autotrophic cultivations of *C. necator* under nitrogen depletion. Heterologous mevalonate formation under the P_{Bad} promoter continued product formation even during the stationary phase, and the same was observed for α-humulene formation under the P_{Rham} promoter, both molecules relying on acetoacetyl-CoA as precursor (Krieg et al., 2018, Garavaglia et al., 2024). In contrast, heterologous acetoin formation in *C. necator* under heterotrophic conditions obtained higher product formation with the P_{Bad} and P_{Rham} promoters compared to the constitutive native P_{phb} promoter, while the inducible promoter showed only minimal product formation in autotrophy (Windhorst, 2019, Windhorst and Gescher, 2019). However, as acetoin formation is not growth-dependent, different promoter efficiencies in dependence of the substrate might be not due to the same mechanisms as observed here.

One potential explanation for the observed differences of nitrogen limitation on CO_2 or fructose would be the metabolic burden imposed by plasmid expression. Upon induction, the heterologous production machinery would compete with the stringent response for cellular resources and protein allocation. Under autotrophic conditions, cells already experience oxidative stress, which is further exacerbated by the sudden expression of a cell-toxic heterologous product (Hoffmann and Rinas, 2004, Schwartz et al., 2009). Additionally, major changes of the metabolism of *R. eutropha* H16 have been observed in autotrophic conditions compared to heterotrophic growth on succinate (Kohlmann et al., 2011), potentially limiting the capacity for heterologous protein production.

Based on the sudden nature of stopped product formation, a link to regulation processes related to the stringent response might play a role and differences in the heterotrophic and autotrophic metabolism might lead to unexpected promoter behaviour. For example, the σ^{54} factor RpoN, responsible for de-repressing the hydrogenases genes and regulating the nitrogen starvation response, plays a significant role during autotrophic growth, while its deletion increased fitness during growth on fructose (Jahn et al., 2024). Its expression is furthermore linked with PHB formation (Tang et al., 2022). Additionally, distinct preferences for the household factors RpoD1 or RpoD2 have been found in the heterotrophic and autotrophic metabolism (Kohlmann et al., 2011). Under autotrophic conditions, furthermore a general upregulation of *phaA*, coding for the first enzyme in PHA-synthesis and the initial enzyme in our isopropanol-operon, was found (Kohlmann et al., 2011). Thus, regulatory responses during nitrogen starvation may vary, preventing metabolic adaptation to the sudden induction of a strong promoter in heterotrophic and autotrophic conditions. This underlines the importance of considering various cultivation conditions during strain development and suggests that optimisation under heterotrophic conditions cannot be directly transferred to autotrophy (Salinas et al., 2022). Based on the results obtained, a re-evaluation of available promoters in *C. necator* under autotrophic conditions could be valuable. As an alternative to the sugar inducible promoters in *C. necator*, P_{Gln} was characterised and its potential was shown for autotrophic isopropanol formation. Its independence from an inducing molecule would increase the potential for scaling up (Johnson et al., 2018) while ensuring control of gene expression relative to constitutive promoters. Hence, the strain Re2133/pEG7d was selected for all further cultivations.

3.2. Impact of methane and industrial biogas on growth and isopropanol formation

Biogas typically contains 45–70% CH_4 (Hagen et al., 2001). After supplementing with the necessary oxygen and hydrogen contents for cultivation *C. necator*, a methane concentration of less than 24% was expected from our initial knowledge of the off-gas mix composition. First, cultivations were performed on synthetic gas mixture containing methane. Fig. 3 shows the impact on growth and isopropanol formation of 16% and 24% CH_4 compared to a reference where methane was replaced by nitrogen. The reference process had a slightly shorter lag phase before it became limited in oxygen at around 48 h. The growth rates were $0.12 \pm 0.02\ h^{-1}$ (0% CH_4), $0.10 \pm 0.02\ h^{-1}$ (16% CH_4), and $0.08 \pm 0.01\ h^{-1}$ (24% CH_4), none of which were statistically significant (two-sided *t*-test assuming equal variance, conducted for all three data pairs). Interestingly, the fact that the H_2 contents were lower in these experiments (40–45%) compared to the ones with synthetic gases (78%) did not impact the growth rate of the strain suggesting that even with such low H_2 content growth was not limited by H_2, at least until an OD value of 1. The presence of methane did not negatively impact either product formation, with a final isopropanol concentration of $0.87 \pm 0.06\ g\ L^{-1}$ in the reference, $0.86 \pm 0.07\ g\ L^{-1}$ with 16% CH_4 and $1.13 \pm 0.18\ g\ L^{-1}$ with 24% CH_4.

The gas compositions showed an enrichment of methane due to the consumption of oxygen, hydrogen and carbon dioxide. Since *C. necator* lacks genes for methane metabolism (Pohlmann et al., 2006), variations

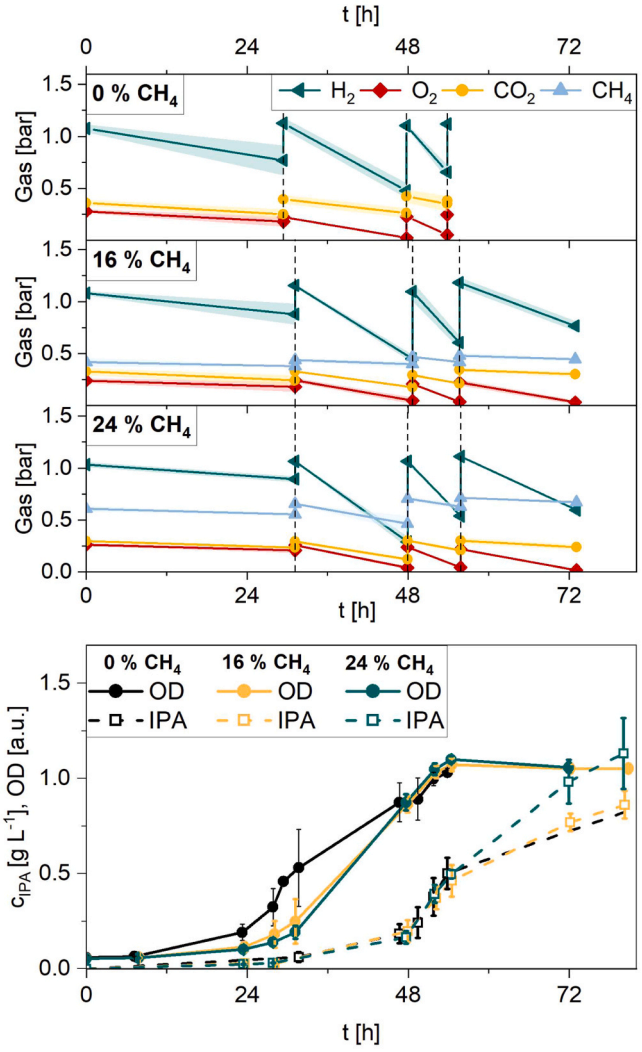

Fig. 3. Autotrophic cultivation of *C. necator* Re2133/pEG7d with synthetic gas mixture containing 0%, 16% or 24% CH_4. All cultivations were conducted with 11–15% CO_2, 40–45% H_2, 8–12% O_2, 0–24% CH_4 and 12–36% nitrogen accordingly. Bottles were filled with the envisaged gas mixture to reach an overpressure of 1.5 bar. All cultivations were conducted in triplicates. The dashed vertical lines indicate gas refills. Upper panel: Measured gas composition of bottle headspace. Shaded areas indicate standard deviation from triplicates. Lower panel: Biomass and isopropanol formation.

in methane partial pressure reflect either measurement inaccuracies in headspace composition or a contamination of the gas sample by residual air in the sampling tube. In the cultivation with 24% methane, the gas phase was replenished four times with a gas mixture containing CH_4/CO_2 in a ratio of 2.2/2.6. Due to the consumption of the other gasses, methane concentrations increased to up to of 46% and CH_4/CO_2-ratios of up to 5.0 were reached. For further improvements, a cultivation system, equipped with an online measurement of dissolved and exhaust gas analysis would allow adaptation of the gas feed to carbon dioxide consumption. With synthetic biogas it was already shown, that purifying a biogas stream to 95% methane is feasible using *C. necator* (Li et al., 2024). The results obtained here further confirm previous publications, describing no negative effect on growth of *C. necator* with up to 50% methane (Li et al., 2024, Serna-García et al., 2024).

After confirming that the presence of methane did not impede product formation, cultivations using landfill biogas were conducted. The landfill biogas used contained 39–43% CH_4, 32–35% CO_2, and

around 3% O_2. Additionally, it contained 10–20 ppm CO and 20 mg m^{-3} siloxanes. The gas was supplemented to 10% oxygen and 50% hydrogen by adding pure gases.

Using biogas as the sole carbon source, 2.0–2.7 g L^{-1} isopropanol were produced with 0.01–0.03 g L^{-1} acetone as by-product (Fig. 4). The obtained product concentrations were higher than those measured for the reference cultivation with synthetic biogas, where an isopropanol concentration of 1.1 ± 0.2 g L^{-1} was obtained. Also, the final isopropanol concentration of 0.87 ± 0.06 g L^{-1} obtained during the cultivation without methane was lower. Furthermore, the lag-phase was shorter in the cultivations using industrial biogas. However, both the reference and the industrial biogas cultivation had an identical maximal growth rate of 0.09 ± 0.02 h^{-1}.

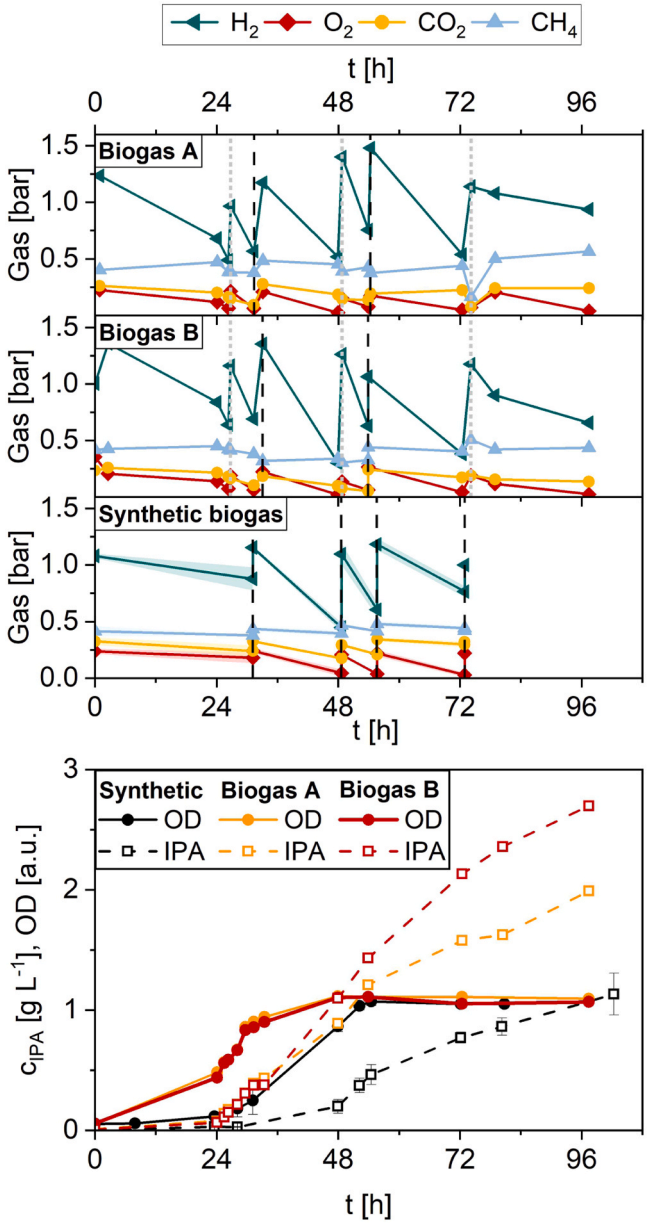

Fig. 4. Growth and isopropanol formation with *C. necator* Re2133/pEG7d with biogas and synthetic biogas as carbon source. The reference cultivation with synthetic biogas was conducted in triplicates, while the cultivation with biogas was conducted in duplicates (A and B). 40% industrial biogas were supplemented with 50% H_2 and 10% O_2. For the synthetic biogas, a composition of 16% CH_4, 12% CO_2, 42% H_2, 10% O_2 and 20% N_2 was targeted. Upper panel: Measured gas composition of the bottle headspace. Vertical black, dashed lines indicate a full refill of the headspace, vertical grey, dotted lines indicate a supplement of 0.6 bar H_2 and 0.2 bar O_2. Upper panel: Measured gas composition of bottle headspace. Shaded areas indicate standard deviation from triplicates for synthetic gas. Lower panel: Biomass and isopropanol formation.

The shorter lag-phase with the industrial gas was surprising and may be attributed to a slightly different gas composition. The biogas cultivations were started with a gas composition of 8–9% O_2, 9–11% CO_2, 16–17% CH_4 and 40–50% H_2 compared to 8–10% O_2, 13–15% CO_2, 15–18% CH_4 and 42–44% H_2 for the reference cultivation. Thus, the reference process had a slightly higher CO_2 concentration. The lag-phase is particularly sensitive to dissolved bicarbonate concentrations that lie outside of the optimal range of 0.66–5.3 mmol L^{-1} (Repaske et al., 1971). With an initial pH of 6.7 and an overpressure of 2.5 bar, a CO_2 concentration of 9% in equilibrium would result in 15 mmol L^{-1} HCO_3^- and 15% CO_2 in 25 mmol L^{-1} HCO_3^-. Thus, the lower CO_2 concentration in the biogas cultivation might explain the shorter lag-phase. To enable a more precise gas feed with lower gas inflow, cultivations have to be conducted at bioreactor scale.

Overall, the conducted cultivations underline the potential of valorising CO_2 in the biogas stream by converting it via the chassis organism *C. necator*. Successful enrichment of methane was shown, with the initial molar CH_4/CO_2-ratio being 1.8 which was increased to 3.8 before the 1st complete refill, 6.6 before the 2nd complete refill and 3.1 by the end of the cultivation.

As biogas potentially contains traces of organic compounds such as volatile fatty acids (VFA), we investigated whether these molecules could provide additional carbon. The start sample of the cultivation was analysed, showing the presence of 1.3 mg L^{-1} acetate, 1.5–1.9 mg L^{-1} isobutyrate, less than 1 mg L^{-1} butyrate, and traces of isovalerate, resulting in a total of around 4 mg L^{-1} VFA. Additionally, non-inoculated cultivations with the biogas mixture were conducted as described in Section 2.3. There, up to 4.7 mg L^{-1} of total VFA after 1.6 h and up to 2.5 mg L^{-1} VFA after 70 h were found in the liquid phase confirming the exchange between liquid and gas phases. With three refills of biogas this sum up to a maximum of 14 mg L^{-1} equalling 0.55 mCmol, which would provide carbon for maximum 11 mg L^{-1} isopropanol. In total, the landfill biogas typically contains around 1.36 mg L^{-1} other volatile organic compounds, showing that only a negligible amount of isopropanol could potentially be formed on these organic compounds.

Nevertheless, the presence of organic compounds might impact lithoautotrophic growth. During co-metabolisation of VFA and CO_2 it was shown, that organic carbon sources were metabolised first, followed by a switch to lithoautotrophic growth (Al-Ani and Kim, 2025). Due to this diauxic behaviour, the lag phase was prolonged when instead of only VFA as carbon sources also CO_2 and H_2 were available, postulating a repression of hydrogenases in the presence of VFA at the used concentration of 10 mM (0.6–1 g L^{-1}). Conversely, a higher production of PHA was observed under mixotrophic conditions compared to heterotrophic cultivation (Jawed et al., 2022). Also, Amer and Kim, (2023) reported faster mixotrophic growth on 1 g L^{-1} acetate and CO_2 rather than using each carbon source separately.

Here, a higher product concentration was obtained on industrial biogas, suggesting a potential positive effect from the presence of organic impurities. In this context, the substrate versatility of *C. necator* is advantageous, making it more flexible than chemical catalysers.

3.3. *Incinerator flue gas as carbon source*

Cultivations were conducted using incinerator flue gas as sole source for carbon dioxide and oxygen. The industrial off-gas contained around 7% CO_2, 14% O_2 and 79% nitrogen (in dry gas), and was supplemented for cultivations with around 40% H_2. In parallel, reference cultivations were conducted, simulating the same gas composition with lab-grade gasses (Fig. 5).

The two reference flasks had shifted lag-phases, with synthetic gas A reaching the maximal OD of 1.0 after 29 h and synthetic gas B after 40 h,

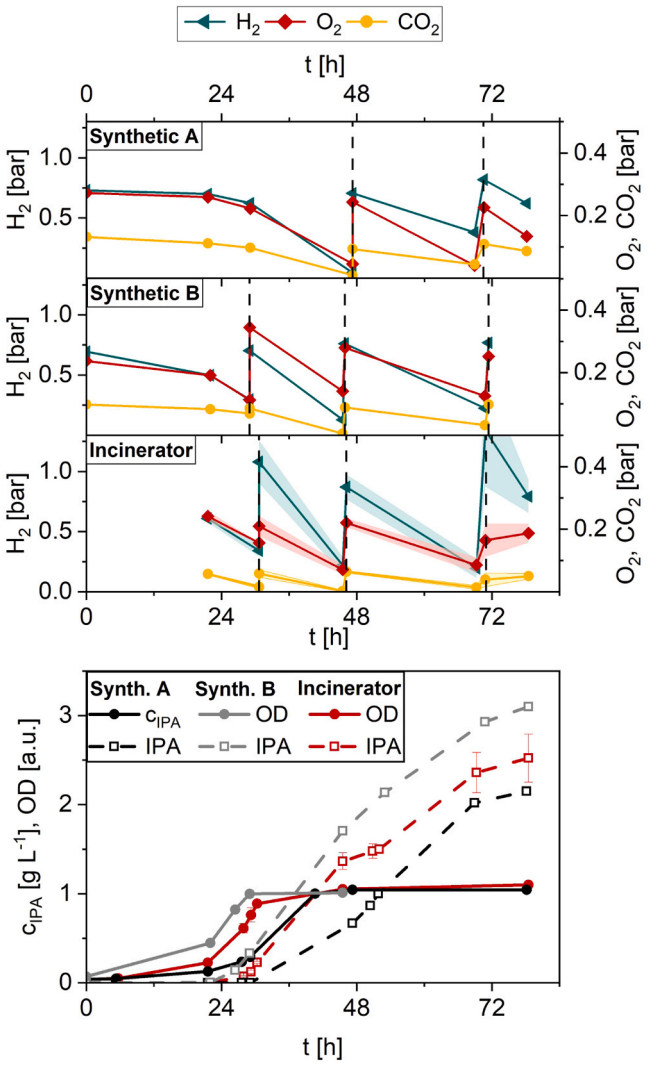

Fig. 5. Growth and isopropanol formation with *C. necator* Re2133/pEG7d with incinerator flue gas and synthetic incinerator gas as the sole carbon source. Reference cultivations are shown in duplicates, cultivations with industrial incinerator flue gas were conducted in triplicates. For the cultivation with industrial incinerator gas, 70% flue gas was supplemented with 30% H_2. Cultivations with synthetic incinerator gas as reference were performed with gas mixture of 56% N_2, 4% CO_2, 30% H_2 and 10% O_2. Vertical black, dashed lines indicate full refill of the headspace Upper panel: Measured gas composition of bottle headspace. Shaded areas indicate standard deviation from triplicates. Lower panel: Biomass and isopropanol formation.

however maximum specific growth rates were similar, 0.12 ± 0.005 h^{-1}. In the cultivation with the shortest lag-phase a higher isopropanol concentration of 3.1 g L^{-1} was observed, compared to 2.2 g L^{-1} in its duplicate, with 0.3 and 0.08 g L^{-1} acetone, respectively. In both, comparable initial gas compositions were obtained with 11% O_2, 5% CO_2, 29% H_2 and 55% N_2 in synthetic gas flask A, 10% O_2, 4% CO_2, 28% H_2 and 58% N_2 in synthetic gas flask B. As observed for the biogas experiments, lowering further the H_2 content (as low as 30% here) in the flasks did not impact the growth rate of the strain pointing out that growth occurred without H_2 limitation. As the flasks were manually baffled, they potentially slightly differed in gas transfer, but without measuring the dissolved gas concentrations, their impact can only be assumed.

The cultivation with incinerator flue gas was conducted in triplicate with a low deviation between the replicates. High growth rates of 0.15 ± 0.02 h^{-1} and a final isopropanol concentration of 2.52 ± 0.27 g L^{-1} with 0.15 ± 0.02 g L^{-1} acetone were obtained. Thus, growth and final product concentration were between both reference flasks. The higher obtained growth rates compared to the previous cultivations might be partially due the lower used liquid volume of 50 mL instead of 100 mL used for cultivations for strain characterisation and compared to biogas cultivations, increasing gas transfer.

Limited to the constraints of the shake flask cultivation system without online gas analysis, the gas feed could not be optimally adapted. However, the cultivation period between 31.2 h and 45.5 h underlines the potential of the process: the head space was refilled with 37% H_2 and 63% incinerator gas, leading to a measured composition of 2.8% CO_2, 8.7% O_2, 42% H_2 and 49% N_2. After 14 h, all of the carbon dioxide was consumed, and the headspace was composed of 85% nitrogen.

The incinerator flue gas was provided from a plant which contains around 94 mg m^{-3} nitric oxide (NO) and 8 mg m^{-3} nitrogen dioxide. In general, nitric oxide is known for inhibiting cytochrome-b oxidases, cause DNA damage, and inhibiting enzymes with Fe-S clusters (Torres et al., 1995, Wink and Mitchell, 1998, Landry et al., 2011). In *C. necator*, nitric oxide and nitrogen dioxide can be used as electron acceptor during anaerobic growth and at least the nitric oxide reductase is also active under aerobic conditions (Kohlmann, 2015, Gemünde et al., 2024). Assuming that all NO dissolves, the four conducted refills could introduce a maximum of 12 mg L^{-1} in total. The incinerator flue gas furthermore contained 5.7 mg m^{-3} carbon monoxide. *C. necator* is quite robust to the presence of CO, even if it cannot metabolise it (Cypionka and Meyer, 1982). In total, 0.002 mg m^{-3} mercury and 0.014 mg m^{-3} other metals were found, mostly zinc but also traces of arsenic and chrome. The found values for chrome and arsenic are well below the concentrations described as growth-inhibiting for *C. necator* H16 while no studies about mercury were found (Akkurt et al., 2023). In contrast, the presence of heavy metals was described to have a positive effect on PHA formation in *Cupriavidus pauculus* KPS 20 and *Cupriavidus taiwanensis* (Pal and Paul, 2012, Chien et al., 2014). In general, PHA formation is upregulated under stress conditions (Obruca et al., 2018) and it is possible that the regulation mechanisms diverting the carbon flux to PHA synthesis under stress conditions also positively impact IPA formation.

Overall, despite the presence of these impurities, no negative effect on growth or product formation was observed. This is in accordance with other studies where industrial off-gas streams were successfully used for cultivation of *C. necator* for PHA production (purified CO_2 from biogas and bioethanol plants (Garcia-Gonzalez and Wever, 2017), raw biogas (Serna-García et al., 2024), bioethanol gas effluent (Rossi et al., 2025)) and for lycopene (exhaust gas of coal-fired power plant (Wu et al., 2022)). Here we have extended the demonstration to the production of a significant quantity (on the order of g/L) of formation of heterologous products from exhaust gases as different as biogas and incineration gas. These results underline the robustness of *C. necator*.

This work demonstrates the potential of producing heterologous, value-added products using the chassis organism *C. necator*. Compared to chemical catalysers this is additionally characterised by a higher tolerance to impurities and flexible product and gas feedstock range (Kim and Chang, 2009, Liew et al., 2013).

4. Summary and conclusion

Gas fermentation with the strain Re2133/pEG7d demonstrated potential to remove CO_2 from industrial gas streams, producing either cleaner offgases containing primarily nitrogen or high-purity methane. Here, we achieved nitrogen enrichment of up to 85% in incineration flue gas or a CH_4/CO_2 ratio of up to 6.6 with biogas. The presence of organic carbon and other impurities did not impair the strain's performance and may even have contributed positively. This study highlights the potential of *C. necator* for transformation industrial offgases.

CRediT authorship contribution statement

I. Weickardt: Conceptualization, Review & Editing, Methodology, Validation, Formal analysis, Investigation, Visualisation, Writing. **A. Zhang:** Validation, Formal analysis, Investigation, Visualisation, Writing. **E. Lombard:** Conceptualization, Review & Editing, Methodology. **E. Grousseau:** Conceptualization, Review & Editing, Methodology. **L.M. Blank:** Resources, Supervision, Administration, Funding acquisition. **C. Chenebault:** Conceptualization, Review & Editing, Resources, Supervision, Administration, Funding acquisition. **B. Percheron:** Resources, Supervision, Administration, Funding acquisition. **N. Gorret:** Conceptualization, Review & Editing, Methodology, Validation, Formal analysis, Investigation, Visualisation, Writing. **S.E. Guillouet:** Conceptualization, Review & Editing, Methodology, Validation, Formal analysis, Investigation, Visualisation, Writing, Resources, Supervision, Administration, Funding acquisition.

Declaration of Competing Interest

The authors declare that they have no known competing financial interests or personal relationships that could have appeared to influence the work reported in this paper.

Acknowledgements

This project has received funding from the European Union's Horizon 2020 research and innovation programme under the Marie Skłodowska-Curie grant agreement No 955740. This work has benefited from a State grant managed by the Agence Nationale de la Recherche under the Investissements d'Avenir programme with the reference ANR-18-EURE-0021. The laboratory of LMB is partially funded by the Deutsche Forschungsgemeinschaft (DFG, German Research Foundation) under Germany's Excellence Strategy—Cluster of Excellence 2186 "The Fuel Science Center" – ID: 390 919 832 and by the Werner Siemens Foundation in the frame of the WSS Research Centre "catalaix".

SG and NG wish to dedicate this article to the memory of Professor A. J. Sinskey for his long-standing support and friendship and for his contribution to the work on PGln.

Appendix A. Supporting information

Supplementary data associated with this article can be found in the online version at doi:10.1016/j.jbiotec.2026.03.005.

Data Availability

Data will be made available on request.

References

Akkurt, Ş., Alkan Uçkun, A., Varınca, K., Uçkun, M., 2023. Ability of *Cupriavidus necator* H16 to resist, bioremove, and accumulate some hazardous metal ions in water. Water Sci. Technol. 87 (12), 3017–3030.

Al-Ani, S., Kim, Y., 2025. Carbon preference by *Cupriavidus necator* for growth and accumulation phases: heterotrophic vs. autotrophic metabolisms. J. Power Sources 626.

Amer, A., Kim, Y., 2023. Minimizing the lag phase of *Cupriavidus necator* growth under autotrophic, heterotrophic, and mixotrophic Conditions. Appl. Environ. Microbiol. 89 (2).

Aouini, I., Ledoux, A., Estel, L., Mary, S., 2014. Pilot plant studies for CO_2 capture from waste incinerator flue gas using MEA based solvent. Oil & Gas. Sci. Technol. Rev. IFP Energ. Nouv. 69 (6), 1091–1104.

Budde, C.F., Riedel, S.L., Willis, L.B., Rha, C., Sinskey, A.J., 2011. Production of poly(3-hydroxybutyrate-co-3-hydroxyhexanoate) from plant oil by engineered *Ralstonia eutropha* strains. Appl. Environ. Microbiol. 77 (9), 2847–2854.

Chien, C.-C., Wang, L.-J., Lin, W.-R., 2014. Polyhydroxybutyrate accumulation by a cadmium-resistant strain of *Cupriavidus taiwanensis*. J. Taiwan Inst. Chem. Eng. 45 (4), 1164–1169.

Cypionka, H., Meyer, O., 1982. Influence of carbon monoxide on growth and respiration of carboxydobacteria and other aerobic organisms. FEMS Microbiol. Lett. 15 (3), 209–214.

Dangel, A.W., Tabita, F.R., 2015. Amino acid substitutions in the transcriptional regulator CbbR lead to constitutively active CbbR proteins that elevate expression of the cbb CO_2 fixation operons in *Ralstonia eutropha* (*Cupriavidus necator*) and identify regions of CbbR necessary for gene activation. Microbiology 161 (9), 1816–1829.

Delamarre, S.C., Batt, C.A., 2006. Comparative study of promoters for the production of polyhydroxyalkanoates in recombinant strains of *Wautersia eutropha*. Appl. Microbiol. Biotechnol. 71 (5), 668–679.

Di Bisceglie, F., García Navarro, J., Lombard, E., Kratzer, R., Kourist, R., Guillouet, S.E., 2025. Conceptual approach for aerobic autotrophic gas cultivation in shake flasks: overcoming the inhibitory effects of oxygen in *Cupriavidus necator*. Biotechnol. J. 20 (2), e202400641.

Fukui, T., Ohsawa, K., Mifune, J., Orita, I., Nakamura, S., 2011. Evaluation of promoters for gene expression in polyhydroxyalkanoate-producing *Cupriavidus necator* H16. Appl. Microbiol. Biotechnol. 89 (5), 1527–1536.

Garavaglia, M., McGregor, C., Bommareddy, R.R., Irorere, V., Arenas, C., Robazza, A., Minton, N.P., Kovacs, K., 2024. Stable Platform for Mevalonate Bioproduction from CO_2. ACS Sustain. Chem. & Eng. 12 (36), 13486–13499.

Garcia-Gonzalez, L., Wever, H. de, 2017. Valorisation of CO_2-rich off-gases to biopolymers through biotechnological process. FEMS Microbiol. Lett. 364 (20).

Gemünde, A., Ruppert, N.-L., Holtmann, D., 2024. Unraveling the electron transfer in *Cupriavidus necator* – Insights into mediator reduction mechanics. ChemElectroChem 11 (14), e202400273.

Gibson, D.G., Yong, L., Chuang, R.Y., Venter, J.C., Hutchinson III, C.A., Simth, H.O., 2009. Enzymatic assembly of DNA molecules up to several hundred kilobases. Nature Meth. 6 (5), 343–347.

Grousseau, E., Lu, J., Gorret, N., Guillouet, S.E., Sinskey, A.J., 2014. Isopropanol production with engineered *Cupriavidus necator* as bioproduction platform. Appl. Microbiol. Biotechnol. 98 (9), 4277–4290.

Hagen, M., Polman, E., Jensen, J.K., Myken, A., Joensson, O., Dahl, A., 2001. Adding gas from biomass to the gas grid, Report SGC 118. ⟨https://www.osti.gov/etdeweb/biblio/20235595⟩.

Hoffmann, F., Rinas, U., 2004. Stress induced by recombinant protein production in *Escherichia coli*. Adv. Biochem. Eng. /Biotechnol. 89, 73–92.

Inokuma, K., Liao, J.C., Okamoto, M., Hanai, T., 2010. Improvement of isopropanol production by metabolically engineered *Escherichia coli* using gas stripping. J. Biosci. Bioeng. 110 (6), 696–701.

Jahn, M., Crang, N., Gynnå, A.H., Kabova, D., Frielingsdorf, S., Lenz, O., Charpentier, E., Hudson, E.P., 2024. The energy metabolism of *Cupriavidus necator* in different trophic conditions. Appl. Environ. Microbiol. 90 (10).

Jawed, K., Irorere, V.U., Bommareddy, R.R., Minton, N.P., Kovács, K., 2022. Establishing Mixotrophic Growth of *Cupriavidus necator* H16 on CO_2 and Volatile Fatty Acids. Fermentation 8 (3), 125.

Johnson, A.O., Gonzalez-Villanueva, M., Tee, K.L., Wong, T.S., 2018. An Engineered Constitutive Promoter Set with Broad Activity Range for *Cupriavidus necator* H16. ACS Synth. Biol. 7 (8), 1918–1928.

Jugder, B.-E., Welch, J., Braidy, N., Marquis, C.P., 2016. Construction and use of a *Cupriavidus necator* H16 soluble hydrogenase promoter (P_{SH}) fusion to gfp (green fluorescent protein). Peer J. 4, e2269.

Kim, D., Chang, I.S., 2009. Electricity generation from synthesis gas by microbial processes: CO fermentation and microbial fuel cell technology. Bioresour. Technol. 100 (19), 4527–4530.

Kircher, M., Schwarz, T., 2023. CO_2 and CO as Feedstock. Springer International Publishing, Cham, p. 412.

Kohlmann, Y., 2015. Charakterisierung des Proteoms von *Ralstonia eutropha* H16 unter lithoautotrophen und anaeroben Bedingungen. Humboldt-Universität zu Berlin, Lebenswissenschaftliche Fakultät.

Kohlmann, Y., Pohlmann, A., Otto, A., Becher, D., Cramm, R., Lütte, S., Schwartz, E., Hecker, M., Friedrich, B., 2011. Analyses of soluble and membrane proteomes of *Ralstonia eutropha* H16 reveal major changes in the protein complement in adaptation to lithoautotrophy. J. Proteome Res. 10 (6), 2767–2776.

Kovach, M.E., Elzer, P.H., Hill, D.S., Robertson, G.T., Farris, M.A., Roop, R.M., Peterson, K.M., 1995. Four new derivatives of the broad-host-range cloning vector pBBR1MCS, carrying different antibiotic-resistance cassettes. Gene 166 (1), 175–176.

Krieg, T., Sydow, A., Faust, S., Huth, I., Holtmann, D., 2018. CO_2 to Terpenes: autotrophic and electroautotrophic α-humulene production with *Cupriavidus necator*. Angew. Chem. Int. Ed. 57 (7), 1879–1882.

Landry, A.P., Duan, X., Huang, H., Ding, H., 2011. Iron-sulfur proteins are the major source of protein-bound dinitrosyl iron complexes formed in *Escherichia coli* cells under nitric oxide stress. Free Radic. Biol. & Med. 50 (11), 1582–1590.

Li, R., Jiang, Y., Huang, J., Luo, K., Fan, X., Guo, R., Liu, T., Zhang, Y., Fu, S., 2024. Simultaneous biogas upgrading and single cell protein production using hydrogen oxidizing bacteria. Chem. Eng. J. 490 (17), 151576.

Liew, F.M., Kopke, M., Dennis, S., 2013. Gas Fermentation for Commercial Biofuels Production. In: Fang, Z. (Ed.), Liquid, Gaseous and Solid Biofuels - Conversion Techniques. IntechOpen.

Liew, F.M., Nogle, R., Köpke, M., 2022. Carbon-negative production of acetone and isopropanol by gas fermentation at industrial pilot scale. Nat. Biotechnol. 40, 335–344.

Logsdon, J.E., Loke, R.A., 2000. Isopropyl Alcohol. Kirk-Othmer Encyclopedia of Chemical Technology. John Wiley & Sons, Ltd.

Lu, J., Brigham, C.J., Gai, C.S., Sinskey, A.J., 2012. Studies on the production of branched-chain alcohols in engineered *Ralstonia eutropha*. Appl. Microbiol. Biotechnol. 96 (1), 283–297.

Lütte, S., Pohlmann, A., Zaychikov, E., Schwartz, E., Becher, J.R., Heumann, H., Friedrich, B., 2012. Autotrophic production of stable-isotope-labeled arginine in *Ralstonia eutropha* strain H16. Appl. Environ. Microbiol. 78 (22), 7884–7890.

Mohammadi, M., Najafpour, G.D., Younesi, H., Lahijani, P., Uzir, M.H., Mohamed, A.R., 2011. Bioconversion of synthesis gas to second generation biofuels: A review. Renew. Sustain. Energy Rev. 15 (9), 4255–4273.

Nagappan, S., Tsai, P.-C., Devendran, S., Alagarsamy, V., Ponnusamy, V.K., 2020. Enhancement of biofuel production by microalgae using cement flue gas as substrate. Environ. Sci. Pollut. Res. 27 (15), 17571–17586.

Obruca, S., Sedlacek, P., Koller, M., Kucera, D., Pernicova, I., 2018. Involvement of polyhydroxyalkanoates in stress resistance of microbial cells: biotechnological consequences and applications. Biotechnol. Adv. 36 (3), 856–870.

Pal, A., Paul, A.K., 2012. Accumulation of polyhydroxyalkanoates by Rhizobacteria underneath Nickel-hyperaccumulators from serpentine ecosystem. J. Polym. Environ. 20 (1), 10–16.

Patricio, J., Angelis-Dimakis, A., Castillo-Castillo, A., Kalmykova, Y., Rosado, L., 2017. Method to identify opportunities for CCU at regional level — Matching sources and receivers. J. CO2 Util. 22, 330–345.

Pohlmann, A., Fricke, W.F., Reinecke, F., Kusian, B., Liesegang, H., Cramm, R., Eitinger, T., Ewering, C., Pötter, M., Schwartz, E., Strittmatter, A., Voss, I., Gottschalk, G., Steinbüchel, A., Friedrich, B., Bowien, B., 2006. Genome sequence of the bioplastic-producing "Knallgas" bacterium *Ralstonia eutropha* H16. Nat. Biotechnol. 24 (10), 1257–1262.

Repaske, R., Ambrose, C.A., Repaske, A.C., Lacy, M.L. de, 1971. Bicarbonate requirement for elimination of the lag period of *Hydrogenomonas eutropha*. J. Bacteriol. 107 (3), 712–717.

Rosenberg, E., DeLong, E.F., Lory, S., Stackebrandt, E., Thompson, F. (Eds.), 2013. The prokaryotes: Applied bacteriology and biotechnology, 4. ed. ed. SpringerLink Bücher. Springer, Berlin, Heidelberg, p. 394.

Rossi, T.S., Francescato, L., Gupte, A.P., Favaro, L., Treu, L., Campanaro, S., 2025. Harnessing the potential of *Cupriavidus necator* for CO_2 capture from alcoholic fermentation and its bioconversion into poly(3-hydroxybutyrate). Bioresour. Technol. 419, 132060.

Salinas, A., McGregor, C., Irorere, V., Arenas-López, C., Bommareddy, R.R., Winzer, K., Minton, N.P., Kovács, K., 2022. Metabolic engineering of *Cupriavidus necator* H16 for heterotrophic and autotrophic production of 3-hydroxypropionic acid. Metab. Eng. 74, 178–190.

Schroeckh, V., Kujau, M., Knüpfer, U., Wenderoth, R., Mörbe, J., Riesenberg, D., 1996. Formation of recombinant proteins in *Escherichia coli* under control of a nitrogen regulated promoter at low and high cell densities. J. Biotechnol. 49 (1-3), 45–58.

Schwartz, E., Voigt, B., Zühlke, D., Pohlmann, A., Lenz, O., Albrecht, D., Schwarze, A., Kohlmann, Y., Krause, C., Hecker, M., Friedrich, B., 2009. A proteomic view of the facultatively chemolithoautotrophic lifestyle of *Ralstonia eutropha* H16. Proteomics 9 (22), 5132–5142.

Schwarze, A., Kopczak, M.J., Rögner, M., Lenz, O., 2010. Requirements for construction of a functional hybrid complex of photosystem I and NiFe-hydrogenase. Appl. Environ. Microbiol. 76 (8), 2641–2651.

Serna-García, R., Silvia Morlino, M., Bucci, L., Savio, F., Favaro, L., Morosinotto, T., Seco, A., Bouzas, A., Campanaro, S., Treu, L., 2024. Biological carbon capture from biogas streams: Insights into *Cupriavidus necator* autotrophic growth and transcriptional profile. Bioresour. Technol. 399, 130556.

Srinivasan, S., Barnard, G.C., Gerngross, T.U., 2002. A novel high-cell-density protein expression system based on *Ralstonia eutropha*. Appl. Environ. Microbiol. 68 (12), 5925–5932.

Sydow, A., Pannek, A., Krieg, T., Huth, I., Guillouet, S.E., Holtmann, D., 2017. Expanding the genetic tool box for Cupriavidus necator by a stabilized L-rhamnose inducible plasmid system. J. Biotechnol. 263, 1–10.

Tang, R., Peng, X., Weng, C., Han, Y., 2022. The Overexpression of phasin and regulator genes promoting the synthesis of polyhydroxybutyrate in *Cupriavidus necator* H16 under nonstress conditions. Appl. Environ. Microbiol. 88 (2), e0145821.

Torres, J., Darley-Usmar, V., Wilson, M.T., 1995. Inhibition of cytochrome c oxidase in turnover by nitric oxide: mechanism and implications for control of respiration. Biochem. J. 312 (Pt 1), 169–173 (Pt 1).

Volova, T.G., Voinov, N.A., 2004. Study of a *Ralstonia eutropha* culture producing polyhydroxyalkanoates on products of coal processing. Appl. Biochem. Microbiol. 40 (3), 249–252.

Warringa, G., 2021. Waste Incineration under the EU ETS. ⟨https://klimaatweb.nl/wp-content/uploads/po-assets/596930.pdf⟩. Accessed 02/2025.

Weickardt, I., Lombard, E., Zhang, A., Blank, L., Guillouet, S.E., 2025. Comparative characterisation of autotrophic and heterotrophic isopropanol formation by Cupriavidus necator in shake flasks. J. Biotechnol. 403, 1–8.

,Weickardt, 2025. Ph.D. Thesis, Université de Toulouse, Toulouse, France, 2025. Overcoming bottlenecks in aerobic gas fermentation : Lessons from CO2-based isopropanol formation by Cupriavidus necator. Available online: https://theses.hal.science/tel-05407638v1 (accessed on 09 December 2025).

Windhorst, C., 2019. Produktion von Plattformchemikalien auf Zucker- und CO_2-Basis mit dem Knallgasbakterium *Cupriavidus necator* H16. Dissertation, KIT.

Windhorst, C., Gescher, J., 2019. Efficient biochemical production of acetoin from carbon dioxide using *Cupriavidus necator* H16. Biotechnol. Biofuels 12 (1), 163.

Wink, D.A., Mitchell, J.B., 1998. Chemical biology of nitric oxide: Insights into regulatory, cytotoxic, and cytoprotective mechanisms of nitric oxide. Free Radic. Biol. Med. 25 (4-5), 434–456.

Wu, H., Pan, H., Li, Z., Liu, T., Liu, F., Xiu, S., Wang, J., Wang, H., Hou, Y., Yang, B., Lei, L., Lian, J., 2022. Efficient production of lycopene from CO_2 via microbial electrosynthesis. Chem. Eng. J. 430, 132943.